

# **Signature of the transition zone in the tomographic results extracted through the eigenfunctions of the two-point correlation**

**S. Balachandar**

**Department of Theoretical and Applied Mechanics**

**University of Illinois, Urbana, IL 61801.**

## **Abstract**

Seismic tomography (Tanimoto 1990, Su & Dziewonski 1991 and Masters *et al.* 1992) has provided detailed three-dimensional map of the shear wave velocity in the Earth's mantle. These tomographic results when characterized by the radial correlation function (Jordan 1993) shows no signature of the mantle transition zone. The radial correlation function and associated radial correlation length are arbitrary subsets of the entire two-point correlation and therefore here we propose an optimal characterization of the two-point correlation in terms of its eigenfunctions. It is shown that the eigenrepresentation of the tomographic data converges rapidly and that the two most energetic eigenfunctions, which nearly account for 54% of the two-point correlation, clearly reveal the signature of the mantle transition zone. These results on the eigenfunctions support the theory that the present day mantle is partially layered.

## I. Introduction

In the last ten years there has been a great increase in the number of mantle convection simulations (Honda *et al.* 1993, Tackley *et al.* 1993, Tackley 1994, Balachandar *et al.* 1994, Peltier & Solheim 1992, among many others). These simulations unlike their predecessors progressively employ more realistic physics such as, internal phase transitions, temperature-dependent viscosity, viscous and adiabatic heatings, etc. These added effects have been shown to have a profound effect on the style of convection. A crucial check for gauging the importance of these various effects is comparison with actual surface observations. Seismic tomography through its detailed probing of the Earth's interior has provided a map of the seismic wave speed to sufficient accuracy that comparison can be made with temperature fields obtained from mantle convection models. Owing to the complex spatio-temporal behavior of the mantle convection, a direct comparison of the strongly time-dependent three-dimensional temperature field obtained in the models with the present day tomographic snapshot of the Earth is not straight forward. Various simple characterizations of thermal convection have been introduced in the past: angular power spectrum (Jarvis & Peltier 1986), root mean square temperature fluctuations (Honda 1987) and normalized vertical mass flux (Steinbach & Yuen 1992). Recently Jordan and coworkers (Jordan *et al.* 1993, Puster & Jordan 1994 and Puster *et al.* 1994) have introduced the two-point correlation as a means of characterizing mantle convection and comparison with tomographic results. Based on radial correlation and associated correlation length it appears that the tomographic models do not exhibit any evidence of the presence of the mantle transition zone, whereas mantle convection models which include the transition zone in their computation show distinctive reduction in the radial correlation at the transition zone. Here we compute the eigenfunctions of the two-point correlation obtained from the tomographic model of the Harvard group (Su *et al.* 1994) and demonstrate that the energetic modes of the tomographic two-point correlation does indeed show clear evidence of decrease in correlation at the transition zone.

## II. Two-point Correlation and Eigenfunction Decomposition

A number of tomographic models have been proposed in the past (Tanimoto 1990, Su & Dziewonski 1991 and Masters *et al.* 1992) that provide a three-dimensional map of the shear wave velocity in the Earth's mantle by inverting the seismic data. Although these models differ in certain respect they all provide the three-dimensional structure of mantle shear-wave velocity heterogeneity, expressed in spherical coordinates as  $\delta v(r, \theta, \phi)$ . Although, these heterogeneities are due to thermal, compositional and phase variations in the mantle material, the thermal effects are assumed to dominate and therefore the tomographic results can be interpreted as related to the present day snap-

shot of the temperature field in the Earth's convecting interior. Normalized two-point correlation function can then be defined as (Jordan *et al.* 1993 and Puster *et al.* 1994):

$$S(r, r^*, \psi) = \frac{\int_0^{2\pi} \int_0^\pi \overline{\delta v(r, \theta, \phi) \delta v(r^*, \theta^*, \phi^*)} d\Omega}{\sigma(r) \sigma(r^*)} \quad (1)$$

where  $d\Omega = \sin \theta d\theta d\phi$ , defines the elementary solid angle and therefore the integral in  $\theta$  and  $\phi$  is over a sphere. The overbar indicates an average over all possible  $\theta^*$  and  $\phi^*$  combination such that the included angle between  $(\theta, \phi)$  and  $(\theta^*, \phi^*)$  is  $\psi$ . The root mean square shear velocity,

$\sigma(r) = \left[ \int_0^{2\pi} \int_0^\pi \delta v^2(r, \theta, \phi) d\Omega \right]^{1/2}$  is used as the normalization factor. The above definition of the two-point correlation assumes that the underlying shear velocity statistics is spherically symmetric. Due to the assumed spherical symmetry,  $S(r, r^*, \psi) = S(r^*, r, \psi)$  and  $S(r, r^*, \psi) = S(r, r^*, -\psi)$ . The correlation function is also intrinsically periodic in angular separation,  $\psi$ , and therefore, the complete information on the two-point statistics can be constructed from its definition on a sub-domain of  $r_{cmb} \leq r \leq r^* \leq r_{moho}$  and  $0 \leq \psi \leq \pi$ , where  $r_{cmb}$  is the radius of the core-mantle boundary and  $r_{moho}$  is the radius of Moho discontinuity.

The two-point correlation contains the complete spatial information of the underlying statistics up to the second order. But its dependence on three independent variables makes it data intensive and therefore it does not provide a compact characterization of the tomographic or convection data. The dependence of the two-point correlation can be reduced to two variables by restricting attention to only its subsets such as the radial correlation,  $B(r, r^*) = S(r, r^*, 0)$  and angular correlation functions,  $A(r, \psi) = S(r, r, \psi)$  (Jordan *et al.* 1993 and Puster *et al.* 1994). Further reduction can be achieved by defining the radial correlation length,  $\varrho_x(r)$ , defined implicitly as,  $B(r - \varrho_x/\sqrt{2}, r + \varrho_x/\sqrt{2}) = x$ , and the correlation angle,  $\Delta_x(r)$ , defined as,  $A(r, \Delta_x) = x$ . The correlation length and angle are insensitive to the actual value of  $x$  and following Jordan *et al.* (1993) we choose  $x=0.75$ .

Purely radial and angular correlations are arbitrary sub-sets of the entire correlation and provide only a partial characterization of the flow. Proper orthogonal decomposition technique, also known as the empirical eigenfunction technique, provides an objective procedure whereby the maxi-

imum information content of the correlation can be recovered at any desired level of its truncated representation (Schmidt 1907, Karhunen 1946, Loeve 1955, Lumley 1967, Sirovich 1987 & 1991). In this method, the empirical eigenfunctions of the two-point correlation are obtained and the eigenvalues associated with these eigenfunctions measure the mean square energy content in them. Thus ordering the eigensolutions in terms of their eigenvalues provide an optimal orthonormal expansion basis. Eigenvalues,  $\lambda^{(m)}$ , and eigenfunctions,  $\Phi_p^{(m)}$ , of the two-point correlation are defined by:

$$\int_{r_{cmb}}^{r_{moho}} \int_0^{2\pi} S(r, r^*, \psi) \Phi^{(m)}(r^*, \xi^*) dr^* d\xi^* = \lambda^{(m)} \Phi^{(m)}(r, \xi) \quad (2)$$

where  $\psi = \xi^* - \xi$ . The kernel,  $S$ , in the above integral equation is real, symmetric and square integrable. From fundamental theorems of symmetric integral equations (Mikhlin 1957) the eigensolutions have the following nice properties: there is not one but a discrete set of eigensolutions to the above integral equation and they can be numbered by the superscript ( $m$ ); the eigenfunctions form a complete orthonormal set; and the eigenvalues are real and non-negative. Due to intrinsic periodicity along  $\psi$ , the eigenfunctions are simple sinusoids along this direction and can be written as

$\Phi(r, \xi) = \sum_{k=-\infty}^{\infty} \hat{\Phi}^k(r) \exp(ik\xi)$ . The eigenfunctions for the  $k^{\text{th}}$  Fourier mode are then given by

$$\int_{r_{cmb}}^{r_{moho}} \hat{S}^k(r, r^*) \hat{\Phi}^{(k,n)}(r^*) dr^* = \lambda^{(k,n)} \hat{\Phi}^{(k,n)}(r) \quad (3)$$

where  $\hat{S}^k$  are the Fourier coefficients of the two-point correlation. These eigensolutions for all the Fourier modes can be ordered such that for each  $m=1,2,\dots$  etc., there is a corresponding doublet index  $(k,n)$ . By Mercer's theorem (Hochstadt 1973) the following mean square estimate of the two-point correlation can be obtained:

$$\int_0^{2\pi} \int_{r_{cmb}}^{r_{moho}} \int_{r_{cmb}}^{r_{moho}} S^2(r, r^*, \psi) dr dr^* d\psi = \sum_{m=\text{all}} [\lambda^{(m)}]^2 \quad (4)$$

The ordering of the eigenvalues and the optimality of the eigenfunction expansion guarantees the rapid convergence of the eigenfunction expansion in representing the two-point correlation in the mean square sense.

### III. Results and Discussion

Here we consider the tomographic model of Su *et al.* (1994) and present results on its two-point correlation and its eigensolution. In Figure 1 shaded contours of the two point correlation at

zero angular separation (ie. the radial correlation function) is plotted as a function of  $r$  and  $r^*$ . Also shown are contour lines of correlation value equal to 0.75 and by definition the gap between the two contour lines measure twice the radial correlation length. As pointed out by Jordan *et al.* (1993), in this plot the signature of the mantle transition zone is not evident, since the radial correlation length does not show any decorrelation across the 670km phase transition zone. In contrast, the mantle convection simulations with internal phase transitions exhibit a strong decrease in the correlation length across the transition zone (Jordan *et al.* 1993). The near constant radial correlation length of approximate 100km throughout the upper half of the mantle only indicates that every point in the upper mantle remains correlated about 100km vertically above and below. In Fig 1 there is some evidence of negative correlation between the transition zone and the lower half of the mantle. Figures 2a and 2b show the correlation contours for two other angular separations,  $\psi = 15^\circ$  and  $90^\circ$ . At small angular separations as shown in figure 2a, the anticorrelation between the transition zone and the deeper parts of the mantle is still evident. On the other hand when the two points are at  $90^\circ$  then the maximum correlation is attained between the transition zone and the lower portions of the mantle.

In Figures 3a, 3b and 3c the same two-point correlation information is presented differently. Here, the position of one of the points is fixed at a radial location of  $r^*$  in the upper mantle, transition zone, and lower mantle respectively and the position of the second point is varied over the  $r, \psi$  plane. For clarity only results for angular separation less than  $90^\circ$  are presented. From Fig. 3a it is clear that the strongest correlations are limited to when the two points are in the upper mantle and to small (less than  $20^\circ$ ) angular separations. A sharp decrease in the correlation across the transition zone can also be observed. Similarly, from Figure 3c it can be observed that the two points in the lower mantle are well correlated for angular separations less than  $20^\circ$ . Again decorrelation between points in the upper mantle with the fixed point in the lower mantle can be seen. In the transition zone, strong correlations are present only in a narrow region around the transition zone and over small angular separations of less than  $10^\circ$ . Thus the signature of the transition zone is clearly evident in the present day tomographic results. The presence of strong radial correlation even around the transition zone might merely indicate a finite width for the transition zone or an undulating lower-upper mantle boundary. Also a partial layering of the mantle can contribute towards the increased correlation in transition zone. In fact the signature of the transition zone can be observed in the original tomographic results as well (see for example figure 7 of Su *et al.* 1994).

The effect of the transition zone can further be analyzed in a compact manner by investigating the depth-dependent structure of the dominant eigenfunctions of the two-point correlation. The eigenfunctions of the top two most energetic modes are plotted in figure 4 as a function of depth. The most energetic eigenmode corresponds to an angular wavenumber of three ( $k=3$ ) and a sequence of  $n=1$ . This single mode accounts for nearly 34% of the informational content of the two-point correlation in the mean square sense (ie.,  $\lambda^{(1)} / \sum \lambda^{(m)} = 0.34$ ). The second most energetic eigenfunction is the  $k=2, n=1$  mode and it represents 20% of the mean square two-point correlation. The third most energetic eigenfunction is a pure radial mode with zero angular wavenumber ( $k=0, n=1$ ) and it captures 12% of the mean square two-point correlation. Together the first three modes account for nearly 66% of the two-point correlation. In fact the first ten eigenmodes account for nearly 86.5% of the two-point correlation and only 40 eigenmodes are necessary to represent the two-point correlation to 99% accuracy in the mean square sense. It can be seen that the top most energetic eigenfunction ( $\phi^{(3,1)}$ ) is positive in the upper and lower mantle but becomes almost zero in the transition zone. The second most energetic eigenfunction ( $\phi^{(2,1)}$ ) is negative near the transition region while being positive in the upper and lower mantle. From Mercer's theorem the two-point correlation can be written in terms of the eigenfunctions as

$$S(r, r^*, \psi^*) = \sum_k \sum_n \lambda^{(k,n)} \hat{\phi}^{(k,n)}(r) \hat{\phi}^{(k,n)\dagger}(r^*) \exp(ik\psi) \quad (5)$$

where  $\dagger$  indicates complex conjugate. Therefore a decrease or reversal of the eigenfunction at the transition zone directly corresponds to a decrease or negative correlation between the transition zone and the upper and the lower mantle. The third most energetic eigenfunction, ( $\phi^{(0,1)}$ ), does not exhibit a change in the eigenstructure near the transition zone. Other higher, less energetic, eigenfunctions do not necessarily exhibit a change in their structure near the transition.

The structure of the two most dominant eigenfunctions suggest a state of layered convection in the present day mantle. Whereas the third most energetic eigenfunction suggests a whole mantle convection and similarly most of the higher, less energetic, eigenfunctions indicate whole mantle convection as well. Based on these results it can be argued that the present day tomographic results support neither completely layered mantle nor a completely whole mantle convection and therefore suggest a partially layered state of convection. Moreover, as evident from the two dominant eigenfunctions, the signature of the transition zone extends over a finite depth and these effects could explain the lack of significant decrease in the radial correlation near the transition zone.

#### IV. Conclusions

The following conclusions can be drawn from the results presented in this letter: (1) The radial correlation along with the radial correlation length (Jordan *et al.* 1993 and Puster *et al.* 1994) provide only a partial characterization of the complete two-point correlation. For example, the subtle signature of the transition zone in the tomographic results of Su *et al.* (1994) is not evident in the radial correlation. (2) The eigenfunctions of the two-point correlation provide an efficient way to optimally characterize the tomographic results. The first ten most energetic eigenfunctions obtained from the SH12/WM13 tomographic model (Su *et al.* 1994) are sufficient to represent the two-point correlation to nearly 86.5% accuracy in the mean square sense. (3) The two most dominant eigenfunctions, which nearly account for 54% of the two-point correlation, clearly reveal the signature of the transition zone in the tomographic results. (4) Based on these eigenfunctions it can be argued that the present day tomographic results suggest a partially layered mantle convection.

#### Acknowledgements

This research has been supported by Division of Mathematical Sciences of the National Science Foundation (NSF DMS 92-01042) under Geo-Math collaboratory program. The author would like to acknowledge Dr. D.A. Yuen for the fruitful discussions which lead towards this work.

#### References

- Balachandar, S., D. A. Yuen, and D.M. Reuteler "High Rayleigh number convection at infinite Prandtl number with temperature-dependent viscosity", TAM report 761, also submitted to *Phys. Fluids*. 1994.
- Hochstadt, H., *Integral Equations*, John Wiley & Sons, New York, 1973.
- Honda, S., The RMS residual temperature in the convecting mantle and seismic heterogeneities, *J. Phys. Earth.*, **35**, 195, 1987.
- Honda, S., D.A. Yuen, S. Balachandar, and D. Reuteler, Three-dimensional instabilities of mantle convection with multiple phase transitions, *Science*, **259**, 1308, 1993.
- Jarvis, G.T., and W.R. Peltier, Lateral heterogeneities in the convecting mantle, *J. Geophys. Res.*, **91**, 435, 1986.
- Jordan, T.H., P. Puster, G.A. Glatzmaier, and P.J. Tackley, Comparisons of seismic earth structures and mantle flow models using radial correlation functions, *Science*, **261**, 1427, 1993.
- Karhunen, K., Zur Spekraltheorie stochasticher, *Prozesse Ann. Acad. Sci. Fennicae*, **37**, 1946.
- Loeve, M.M., *Probability Theory*, Van Nostrand, Princeton, N.J. 1955.
- Lumley, J.L., The structure of inhomogeneous turbulent flows. In *Atmospheric turbulence and radio wave propagation*. ed: A.M. Yaglom and V.I. Tatarski, Moscow, 166, 1967.

- Masters, G., H. Bolton and P. Shearer, Large-scale 3D structure of the mantle, *EOS Trans. AGU.*, **73**, Spring Meeting Suppl., 201, 1992.
- Mikhlin, S.G., *Integral Equations*, Pergmon Press, New York, 1957.
- Peltier, W.R., and L.P. Solheim, Mantle phase transitions and layered chaotic convection, *Geophys. Res. Lett.*, **19**, 321, 1992.
- Puster, P., and T.H. Jordan, Stochastic analysis of mantle convection experiments using two-point correlation functions, *Geophys. Res. Lett.*, **21**, 305, 1994.
- Puster, P., T.H. Jordan, and B.H. Hager, The characterization of mantle convection experiments using two-point correlation functions, submitted to *J. Geophys. Res.*, 1994.
- Schmidt, E., Zur theorie der linearen und nichtlinearen integralgleichungen. I teil: entwicklung willkullicher funktion nach systemen vorgeschriebener, *Mathematische Annalen*, **63**, 433, 1907.
- Sirovich, L., Turbulence and the dynamics of coherent structures, *Quart. Appl. Math.*, **XLV**, 561, 1987.
- Sirovich, L., Empirical eigenfunctions and low dimensional systems. In *New perspectives in turbulence*, Springer-Verlag, New York, 1991.
- Steinbach, V., and D.A. Yuen, The effects of multiple phase transitions on Venusian mantle convection, *Geophys. Res. Lett.*, **19**, 2243, 1992.
- Su, W., R.L. Woodward, and A.M. Dziewonski, Degree 12 model of shear velocity heterogeneity in the mantle, *J. Geophys. Res.*, **99**, 6945, 1994.
- Su, W., and A.M. Dziewonski, Predominance of long-wavelength heterogeneity in the mantle, *Nature*, **352**, 121, 1991.
- Tackley, P.J., D.J. Stevenson, G.A. Glatzmaier, and G. Schubert, Effects of an endothermic phase transition at 670 km depth in a spherical model of convection in the Earth's mantle, *Nature*, **361**, 699, 1993.
- Tackley, P.J., Effects of strongly temperature-dependent viscosity on time- dependent, three-dimensional models of mantle convection, *Geophys. Res. Lett.*, **20**, 2187-2190, 1993.
- Tanimoto, T., Long-wavelength S-wave velocity structure throughout the mantle, *Geophys. J. Int.*, **100**, 327-336, 1990.



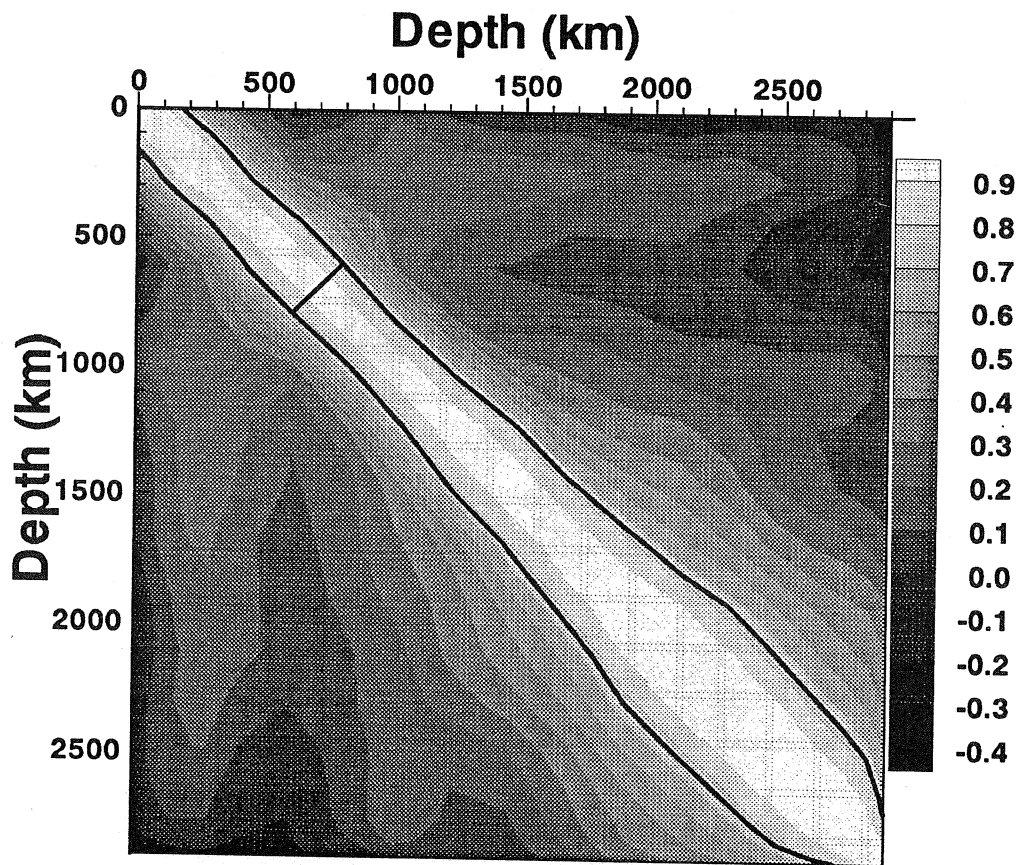


Fig. 1 Contour plot of the two-point correlation of the SH12/WM13 tomographic model (Su *et al.* 1994) at zero angular separation. Also shown in this plot are contour lines of radial correlation equal to 0.75. The normal distance between the two lines measures twice the correlation length, according to the definition given in text. It can be seen that this correlation length remains nearly a constant over most of the mantle.

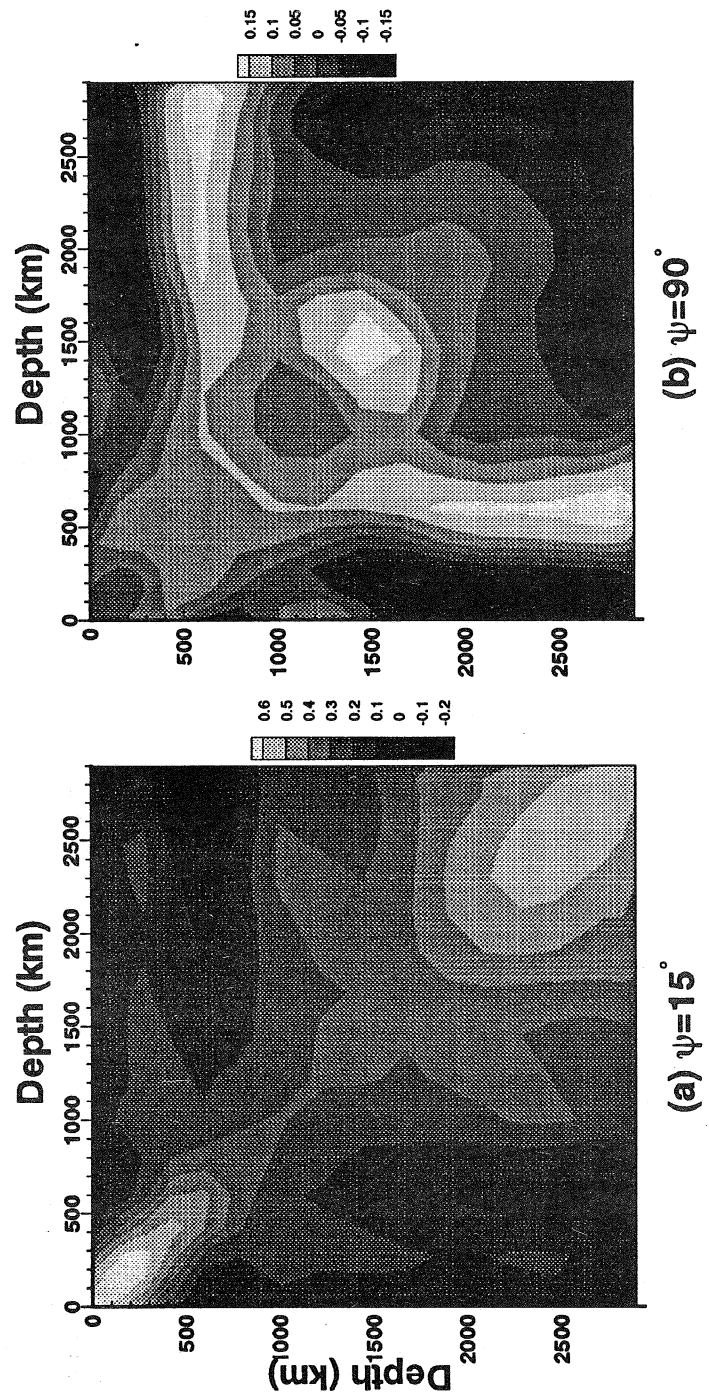


Fig 2. Shaded contours of the two-point correlation of the SH12/WM13 tomographic model (Su *et al.* 1994) at angular separations of 15 and 90 degrees.

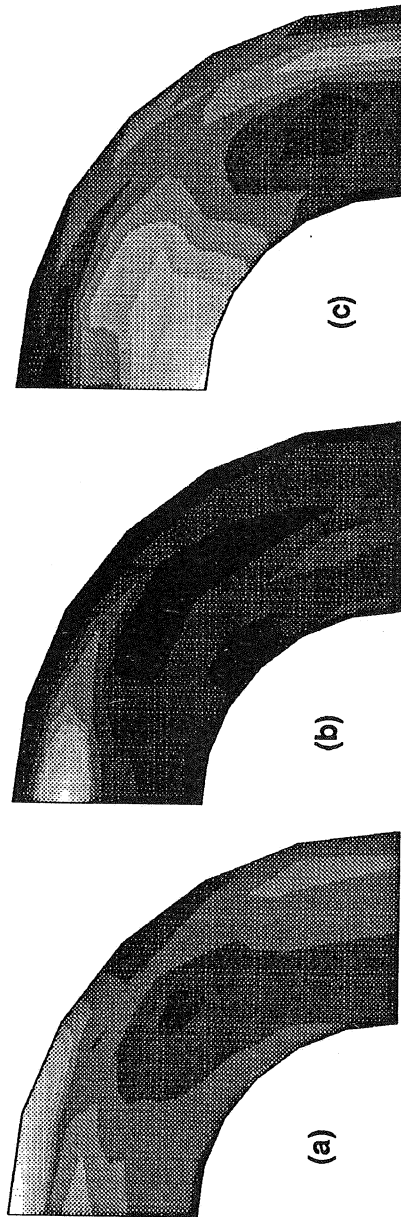


Fig 3. In these three frames the two-point correlations is plotted in such a way that one of the points is at a fixed location of (a) close to the surface; (b) in the transition zone and (c) in the lower mantle. The plots show the shaded contours of the correlation as the position of the second point is varied.

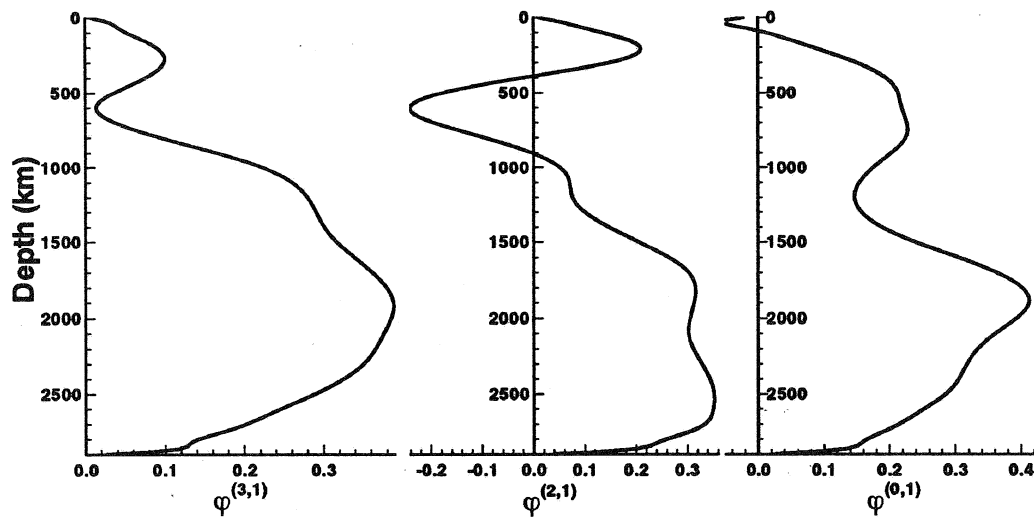


Fig 4. This figure shows the structure of the two most energetic eigenfunctions of the two-point correlation of the SH12/WM13 tomographic model (Su *et al.* 1994). The most energetic eigenfunction corresponds to an angular frequency of 3 and the second most energetic eigenmode corresponds to an angular frequency of 2 and together they account for nearly 50% of of the two-point correlation in the mean square sense.





## List of Recent TAM Reports

| No. | Authors   | Title   | Date       |
|-----|---|---|------------|
| 716 | Sofronis, P.                                      | Linearized hydrogen elasticity  | July 1993  |
| 717 | Nitzsche, V. R., and K. J. Hsia                   | Modelling of dislocation mobility controlled brittle-to-ductile transition  | July 1993  |
| 718 | Hsia, K. J., and A. S. Argon                      | Experimental study of the mechanisms of brittle-to-ductile transition of cleavage fracture in silicon single crystals                 | July 1993  |
| 719 | Cherukuri, H. P., and T. G. Shawki                | An energy-based localization theory: Part II—Effects of the diffusion, inertia and dissipation numbers                                | Aug. 1993  |
| 720 | Aref, H., and S. W. Jones                         | Chaotic motion of a solid through ideal fluid   | Aug. 1993  |
| 721 | Stewart, D. S.                                    | Lectures on detonation physics: Introduction to the theory of detonation shock dynamics   | Aug. 1993  |
| 722 | Lawrence, C. J., and R. Mei                       | Long-time behavior of the drag on a body in impulsive motion  | Sept. 1993 |
| 723 | Mei, R., J. F. Klausner, and C. J. Lawrence       | A note on the history force on a spherical bubble at finite Reynolds number   | Sept. 1993 |
| 724 | Qi, Q., R. E. Johnson, and J. G. Harris           | A re-examination of the boundary layer attenuation and acoustic streaming accompanying plane wave propagation in a circular tube      | Sept. 1993 |
| 725 | Turner, J. A., and R. L. Weaver                   | Radiative transfer of ultrasound  | Sept. 1993 |
| 726 | Yogeswaren, E. K., and J. G. Harris               | A model of a confocal ultrasonic inspection system for interfaces   | Sept. 1993 |
| 727 | Yao, J., and D. S. Stewart                        | On the normal detonation shock velocity-curvature relationship for materials with large activation energy                             | Sept. 1993 |
| 728 | Qi, Q.  | Attenuated leaky Rayleigh waves   | Oct. 1993  |
| 729 | Sofronis, P., and H. K. Birnbaum                  | Mechanics of hydrogen-dislocation-impurity interactions: Part I—Increasing shear modulus  | Oct. 1993  |
| 730 | Hsia, K. J., Z. Suo, and W. Yang                  | Cleavage due to dislocation confinement in layered materials  | Oct. 1993  |
| 731 | Acharya, A., and T. G. Shawki                     | A second-deformation-gradient theory of plasticity  | Oct. 1993  |
| 732 | Michaleris, P., D. A. Tortorelli, and C. A. Vidal | Tangent operators and design sensitivity formulations for transient nonlinear coupled problems with applications to elasto-plasticity | Nov. 1993  |
| 733 | Michaleris, P., D. A. Tortorelli, and C. A. Vidal | Analysis and optimization of weakly coupled thermo-elasto-plastic systems with applications to weldment design                        | Nov. 1993  |
| 734 | Ford, D. K., and D. S. Stewart                    | Probabilistic modeling of propellant beds exposed to strong stimulus  | Nov. 1993  |
| 735 | Mei, R., R. J. Adrian, and T. J. Hanratty         | Particle dispersion in isotropic turbulence under the influence of non-Stokesian drag and gravitational settling                      | Nov. 1993  |
| 736 | Dey, N., D. F. Socie, and K. J. Hsia              | Static and cyclic fatigue failure at high temperature in ceramics containing grain boundary viscous phase: Part I—Experiments         | Nov. 1993  |
| 737 | Dey, N., D. F. Socie, and K. J. Hsia              | Static and cyclic fatigue failure at high temperature in ceramics containing grain boundary viscous phase: Part II—Modelling          | Nov. 1993  |
| 738 | Turner, J. A., and R. L. Weaver                   | Radiative transfer and multiple scattering of diffuse ultrasound in polycrystalline media   | Nov. 1993  |
| 739 | Qi, Q., and R. E. Johnson                         | Resin flows through a porous fiber collection in pultrusion processing  | Dec. 1993  |
| 740 | Weaver, R. L., W. Sachse, and K. Y. Kim           | Transient elastic waves in a transversely isotropic plate   | Dec. 1993  |
| 741 | Zhang, Y., and R. L. Weaver                       | Scattering from a thin random fluid layer   | Dec. 1993  |

(continued on next page)

### List of Recent TAM Reports (cont'd)

| <i>No.</i> | <i>Authors</i>  | <i>Title</i>  | <i>Date</i> |
|------------|---|---|-------------|
| 742        | Weaver, R. L., and W. Sachse  | Diffusion of ultrasound in a glass bead slurry  | Dec. 1993   |
| 743        | Sundermeyer, J. N., and R. L. Weaver  | On crack identification and characterization in a beam by nonlinear vibration analysis  | Dec. 1993   |
| 744        | Li, L., and N. R. Sottos  | Predictions of static displacements in 1-3 piezocomposites  | Dec. 1993   |
| 745        | Jones, S. W.  | Chaotic advection and dispersion  | Jan. 1994   |
| 746        | Stewart, D. S., and J. Yao  | Critical detonation shock curvature and failure dynamics: Developments in the theory of detonation shock dynamics             | Feb. 1994   |
| 747        | Mei, R., and R. J. Adrian   | Effect of Reynolds-number-dependent turbulence structure on the dispersion of fluid and particles                             | Feb. 1994   |
| 748        | Liu, Z.-C., R. J. Adrian, and T. J. Hanratty  | Reynolds-number similarity of orthogonal decomposition of the outer layer of turbulent wall flow                              | Feb. 1994   |
| 749        | Barnhart, D. H., R. J. Adrian, and G. C. Papen  | Phase-conjugate holographic system for high-resolution particle image velocimetry   | Feb. 1994   |
| 750        | Qi, Q., W. D. O'Brien Jr., and J. G. Harris   | The propagation of ultrasonic waves through a bubbly liquid into tissue: A linear analysis                                    | Mar. 1994   |
| 751        | Mittal, R., and S. Balachandar  | Direct numerical simulation of flow past elliptic cylinders   | May 1994    |
| 752        | Anderson, D. N., J. R. Dahlen, M. J. Danyluk, A. M. Dreyer, K. M. Durkin, J. J. Kriegsmann, J. T. McGonigle, and V. Tyagi | Thirty-first student symposium on engineering mechanics, J. W. Phillips, coord.   | May 1994    |
| 753        | Thoroddsen, S. T.   | The failure of the Kolmogorov refined similarity hypothesis in fluid turbulence   | May 1994    |
| 754        | Turner, J. A., and R. L. Weaver   | Time dependence of multiply scattered diffuse ultrasound in polycrystalline media   | June 1994   |
| 755        | Riahi, D. N.  | Finite-amplitude thermal convection with spatially modulated boundary temperatures  | June 1994   |
| 756        | Riahi, D. N.  | Renormalization group analysis for stratified turbulence  | June 1994   |
| 757        | Riahi, D. N.  | Wave-packet convection in a porous layer with boundary imperfections  | June 1994   |
| 758        | Jog, C. S., and R. B. Haber   | Stability of finite element models for distributed-parameter optimization and topology design                                 | July 1994   |
| 759        | Qi, Q., and G. J. Brereton  | Mechanisms of removal of micron-sized particles by high-frequency ultrasonic waves  | July 1994   |
| 760        | Shawki, T. G.   | On shear flow localization with traction-controlled boundaries  | July 1994   |
| 761        | Balachandar, S., D. A. Yuen, and D. M. Reuteler   | High Rayleigh number convection at infinite Prandtl number with temperature-dependent viscosity                               | July 1994   |
| 762        | Phillips, J. W.   | Arthur Newell Talbot—Proceedings of a conference to honor TAM's first department head and his family                          | Aug. 1994   |
| 763        | Man., C. S., and D. E. Carlson  | On the traction problem of dead loading in linear elasticity with initial stress  | Aug. 1994   |
| 764        | Zhang, Y., and R. L. Weaver   | Leaky Rayleigh wave scattering from elastic media with random microstructures   | Aug. 1994   |
| 765        | Cortese, T. A., and S. Balachandar  | High-performance spectral simulation of turbulent flows in massively parallel machines with distributed memory                | Aug. 1994   |
| 766        | Balachandar, S.   | Signature of the transition zone in the tomographic results extracted through the eigenfunctions of the two-point correlation | Sept. 1994  |